Acta Cryst E CRYSTALLOGRAPHIC COMMUNICATIONS

ISSN 2056-9890

Cr_5B_3 with the Shastry–Sutherland lattices

Makoto Tokuda,[a]* Kunio Yubuta,[b] Toetsu Shishido[c] and Kazumasa Sugiyama[c]

[a]Institute of Industrial Nano materials, Kumamoto University, 2-39-1 Kurokami, Chuo-ku, Kumamoto 860-8555, Japan, [b]Institute for Aqua Regeneration, Shinshu University, 4-17-1 Wakasato, Nagano 380-8553, Japan, and [c]Institute for Materials Research, Tohoku University, 2-1-1 Katahira, Aoba-ku, Sendai 980-8577, Japan. *Correspondence e-mail: tokuda@nech.kumamoto-u.ac.jp

Received 14 May 2025
Accepted 18 July 2025

Edited by Y. Ozawa, University of Hyogo, Japan

Keywords: single-crystal diffraction; crystal structure; boride.

CCDC reference: 2473809

Supporting information: this article has supporting information at journals.iucr.org/e

The structural parameters of pentachromium triboride, Cr_5B_3, with Shastry–Sutherland lattices were refined based on single-crystal X-ray diffraction data. Cr_5B_3 crystallizes in the space group *I*4/*mcm* (No. 140), with the following lattice parameters: a = 5.4728 (1) and c = 10.0794 (2) Å. The present study succeeded in refining the positional and anisotropic atomic displacement parameters of the Cr and B atoms.

1. Chemical context

Several intermetallic compounds, such as CrB_4 (orthorhombic, *Immm*), CrB_2 (hexagonal, *P*6/*mmm*), Cr_3B_4 (orthorhombic, *Immm*), CrB (orthorhombic, *Cmcm*), Cr_5B_3 (tetragonal, *I*4/*mcm*), *t*-Cr_2B (tetragonal, *I*4/*mcm*) and *o*-Cr_2B (orthorhombic, *Fddd*), exist in the binary Cr–B system (Lundström, 1969; Guy & Uraz, 1976; Massalski *et al.*, 2016). These binary chromium borides have attracted research attention as high-strength materials with excellent thermal, corrosion, and wear resistance. In addition to synthesis techniques (Okada *et al.*, 1996; Iizumi *et al.*, 1998), their applications in industrial fields have been also developed.

Notable magnetic (Guy, 1976; Leyarovska *et al.*, 1979), thermal (Leyarovska *et al.*, 1979) and transportation (Cruceanu *et al.*, 1975) properties have been reported in more than 130 intermetallic compounds with a Cr_5B_3 prototype (ICSD, 2025). Antiferromagnetic ordering occurs in Cr_5B_3 at T_N = 91.5 K (Leyarovska *et al.*, 1979). The magnetic susceptibility and specific heat measurements of Cr_5B_3 suggest that its magnetic behavior originates from antiferromagnetic spin fluctuations in an itinerant electron system, rather than from localized magnetic moments (Leyarovska *et al.*, 1979). The observed effective magnetic moment of 0.02 μ_B per Cr atom indicates a low-spin state with significant *d*-electron delocalization. These findings imply that the formal oxidation state of Cr lies between +2 and +3. In the Cr_5B_3-type structure, metal atoms locate the two non-equivalent crystallographic sites. A two-dimensional square lattice formed by one of these metal sites can host magnetically frustrated orthogonal dimer systems. This square lattice is classified the Sharstry–Sutherland lattice (SSL; Shastry & Sutherland, 1981; Kageyama *et al.*, 1999; Siemensmeyer *et al.*, 2008; Coleman & Nevidomskyy, 2010). In particular, Ce_5Si_3, which has the Cr_5B_3-type structure, features a bilayer system of the SSL layers formed by Ce atoms, with additional interactions from out-of-plane Ce atoms contributing to its complex magnetic properties. (Ueta *et al.*, 2024).

The first structural investigation of Cr_5B_3 was conducted using a single crystalline sample (Bertaut & Blum, 1953). Both

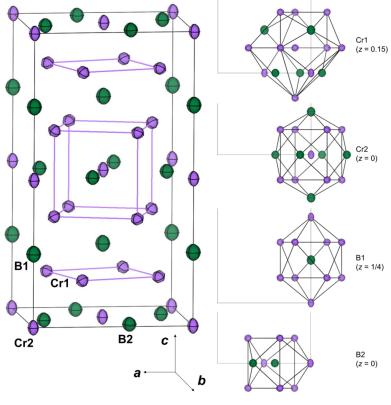

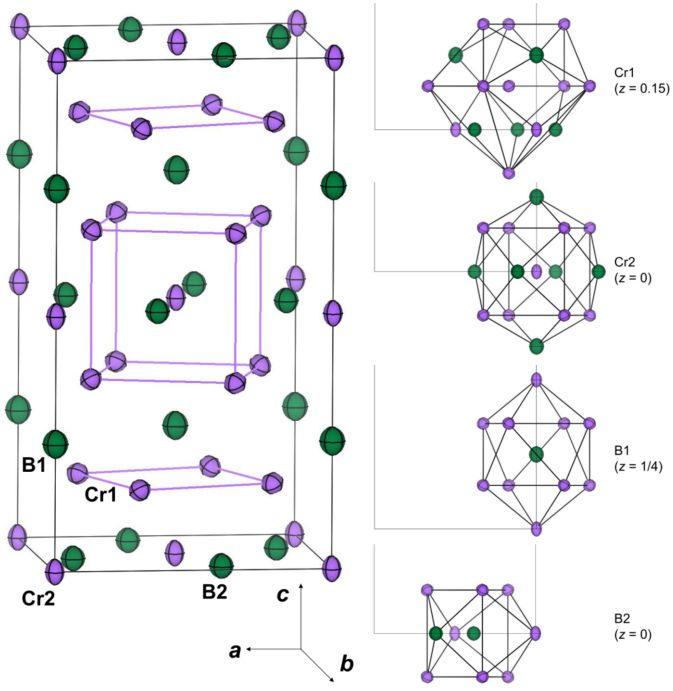

Figure 1
(left) Crystal structures of Cr_5B_3. The purple and green displacement ellipsoids correspond to Cr and B atoms, respectively. Displacement ellipsoids are drawn at the 99% probability level. (right) Coordination polyhedra for each site, $Cr_{11}B_5$ 16-vertex Frank–Kasper cluster around Cr1 on 16*l* site (z = 0.15), Cr_8B_6 rhombic dodecahedron around Cr2 on 4*c* site (z = 0), Cr_{10} bicapped square antiprism around B1 on 4*a* site (z = 1/4), and Cr_8B tricapped trigonal prism around B2 on 8*h* sites (z = 0).

Table 1
Selected bond lengths (Å) in Cr_5B_3.

Cr1:$Cr_{11}B_5$ 16-vertex Frank–Kasper	
Cr1—B2×2	2.1803 (3)
Cr1—B2×1	2.2015 (6)
Cr1—B1×2	2.2826 (1)
Cr1—Cr2×1	2.4218 (4)
Cr1—Cr2×2	2.5072 (2)
Cr1—Cr1×1	2.6513 (3)
Cr1—Cr1×2	2.8098 (1)
Cr1—Cr1×4	2.8688 (1)
Cr1—Cr1×1	2.9468 (5)
Cr2:Cr_8B_6 rhombic dodecahedron	
Cr2—B2×4	2.1903 (4)
Cr2—Cr1×8	2.5072 (1)
Cr2—B1×2	2.5199 (1)
B1:Cr_{10} bicapped square antiprism	
B1—Cr1×8	2.2826 (1)
B1—Cr2×2	2.5199 (1)
B2:Cr_8B tricapped trigonal prism	
B2—B2×1	1.8168 (16)
B2—Cr1×4	2.1802 (3)
B2—Cr2×2	2.1903 (4)
B2—Cr1×2	2.2015 (6)

Cr and B atoms in the tetragonal Cr_5B_3 occupy two different Wyckoff sites, namely, 4*c* (0, 0, 0) and 16*l* (x, $x + \frac{1}{2}$, z) denoted as the Cr2 and Cr1 sites, respectively, and 4*a* (0, 0, 1/4) and 8*h* (x, $x + \frac{1}{2}$, 0) denoted as the B1 and B2 sites, respectively. Subsequent structural studies on Cr_5B_3 have been limited to determining the lattice parameters, and the structural parameters have remained unchanged for over half a century (Portnoi *et al.*, 1969; von Robitsch, 1974; Paradelli & Gianoglio, 1976; Hu *et al.*, 2014). Furthermore, regarding the atomic displacement parameters (ADPs) Bertaut & Blum (1953) did not determine them. Therefore, refining the anisotropic ADPs is essential for a more accurate structural description. Authors have reported that ADPs provide useful information about the structural properties of several metal boride compounds, such as $YCrB_4$ (Tokuda *et al.*, 2022) and *RE*Rh_3B_2 (*RE* = Pr, Nd, and Sm) (Tokuda *et al.*, 2023). In this study, we update the structural parameters of Cr_5B_3 and perform a refinement, including the anisotropic ADPs.

Cr_5B_3-type (called T_2-phase) analogous compounds have been studied using various experimental and theoretical methods, because they have many derivatives of the form M_5XB_2 (M = metal, X = non-metal or semi-metal such as Si, P, and Ge; Dahlqvist & Rosen, 2022). The structures of M_5XB_2 and Cr_5B_3 are related to the order–disorder atomic arrangements, in which M_5XB_2 and X atoms solely occupy the 4*a* site. Recently, several compounds of the form M_5XB_2 have been reported to exhibit superconductivity, such as Ta_5GeB_2 (T_c ~3.8 K; Hadi *et al.*, 2016; Corrêa *et al.*, 2016), Mo_5GeB_2 (T_c = 5.8 K; Ruan *et al.*, 2021), Mo_5SiB_2 (T_c = 5.8 K; Machado *et al.*, 2011), Mo_5PB_2 (T_c = 9 K; McGuire & Parker, 2016), and $(W, Ta)_5SiB_2$ (T_c = 6.5 K; Fukuma *et al.*, 2012).

2. Structural commentary

In the Cr_5B_3 structure, the Cr atoms at the Cr2 and Cr1 sites are surrounded by a Cr_8B_6 rhombic dodecahedron and a $Cr_{11}B_5$ 16-vertex Frank–Kasper cluster, respectively, and those at the B1 and B2 sites are surrounded by a Cr_{10} bicapped square antiprism and Cr_8B tricapped trigonal prism, respectively (Fig. 1).

The B2—B2 interatomic distances on the z = 0 and 1/2 plane is 1.8168 (16) Å, which is significantly longer than the average B—B covalent bond distances of 1.77 Å in rhombohedral boron (Donohue, 1974). This B2 pair (B dimer) serves as a bridging unit between two adjacent Cr–B tricapped trigonal prisms, with each boron atom occupying the center of a respective polyhedron. The Cr—B interatomic distances are in the range of 2.1803 (3)–2.2826 (1) Å (Table 1), which are close to the sum of the Goldschmidt radii (r_{Cr} = 1.36 Å and r_B = 0.97 Å; Brandes & Brook, 1992). The intraplane Cr2···Cr2 and intraplane Cr2···Cr1 distances are 3.8698 (1) and 2.5072 (1) Å, respectively. The interplane Cr2···Cr1 distance is significantly smaller than the sum of the radii of the Cr atoms, and the anisotropic atomic displacement parameters (ADPs) for Cr2 exhibit a larger anisotropy than those of Cr1 (Table 2). The U_{33} of Cr2 is approximately 1.75 times larger than U_{11} (= U_{22}), indicating that the displacement ellipsoid of Cr2 is elongated along the *c*-axis direction. These Cr···Cr distances and ADPs of Cr2 indicate a strong correlation between the Cr2 and Cr1 atoms.

Table 2
Atomic coordinates and anisotropic atomic displacement parameters (10^3 Å^2) for Cr_5B_3.

The Cr atoms lie on the Wyckoff site, the 4*c* site (0, 0, 0) and the 16*l* site (x, $x+\frac{1}{2}$, z), and the B atoms occupy the 4*a* site (0, 0, 1/4) and the 8*h* site (x, $x+\frac{1}{2}$, 0). The anisotropic displacement factor exponent takes the form $2\pi^2[(ha^*)^2U_{11} + \cdots + 2hka^*b^*U_{12}]$. U_{eq} is defined as a third of the trace of the orthogonalized U_{ij} tensor; $U_{11} = U_{22}$, $U_{13} = U_{23}$.

Atom	x	z	U_{11}	U_{33}	U_{12}	U_{13}	U_{eq}
Cr1	0.17128 (2)	0.14618 (2)	0.00396 (2)	0.00369 (4)	−0.00001 (1)	−0.00022 (1)	0.00285 (3)
Cr2	0.0	0.0	0.00312 (6)	0.00547 (4)	0.0	0.0	0.00391 (2)
B1	0.0	0.25	0.00544 (17)	0.0066 (3)	0.0	0.0	0.00583 (12)
B2	0.38263 (10)	0.0	0.00489 (12)	0.0050 (4)	−0.00013 (15)	0.0	0.00492 (8)

The bonding configurations of boron in metal boride compounds (*Mx*B*y*) are classified with the metal-to-boron ratio (*M*:B), and their structural characteristics have been systematically investigated (Rogl & Nowotny, 1978). In metal-rich compositions *M*/B > 1.5, boron typically exists as isolated B or a B–B dimer, occupying localized positions within the metal network. As the metal-to-boron ratio decreases, the bonding motifs transform progressively into mono-periodic chains (*e.g.*, Cr_2AlB_2-type), di-periodic boron layers (*e.g.*, CrB_2-type), and eventually into three-dimensional frameworks constructed from B_6 octahedra or B_{12} icosahedra (*e.g.* UB_4-type). This structural diversity plays a crucial role in determining the electronic structure and physical properties of borides. In particular, Cr_5B_3, with a *M*:B of 5:3 (1.67), is categorized as a metal-rich boride and the boron configurations B1 and B2 sites correspond to 'isolated B' and 'B–B dimer', respectively. The slabs of Cr_8 square antiprisms [Cr···Cr interatomic distances of 2.42178 (14) and 2.86881 (3) Å] together with the B1 site and Cr square lattice [Cr···Cr interatomic distance of 2.50718 (5) Å] with B2 dimers [B2···B2 interatomic distance of 1.8168 (16) Å] alternately stack along the *c*-axis as shown in Fig. 2. The slabs of Cr_8 square antiprisms together with the B1 site connect via edge-sharing. Unlike boron-rich borides, the boron unit, Cr_5B_3, are locally confined, reflecting a characteristic intermetallic bonding framework in which boron can act predominantly as an electron donor.

Fig. 3 depicts the crystal structures of the binary metal borides Cr_5B_3 (*a*, *b*) and TmB_4 (*c*, *d*) viewed along the *c*-axis (*a*, *c*) and *b*-axis (*b*, *d*). The purple, green and blue spheres indicate the Cr, B, and Tm atoms, respectively. The gray squares in (*a*, *c*, *e*, *f*, *g*) are the respective unit cells. Cr lattices [Cr···Cr interatomic distance of 2.6513 (1) and 2.8688 (1) Å] at z = 0.15 (Fig. 3*e*) and z = 0.35 (Fig. 3*f*) in the slabs of Cr_8

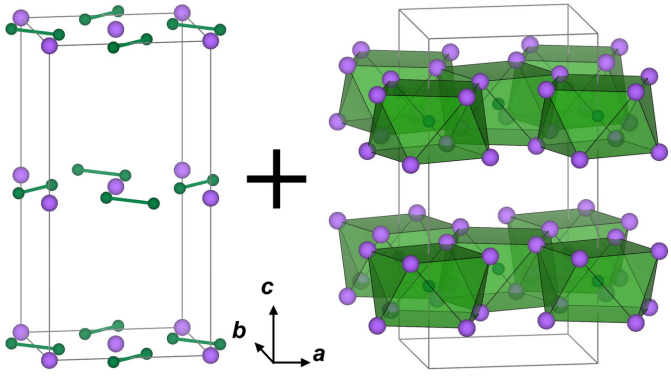

Figure 2
(left) Cr square lattices with B dimers at z = 0 and z = 1/2, and (right) slabs of Cr_8B square antiprisms around the B1 site between z = 0.15 and z = 0.35.

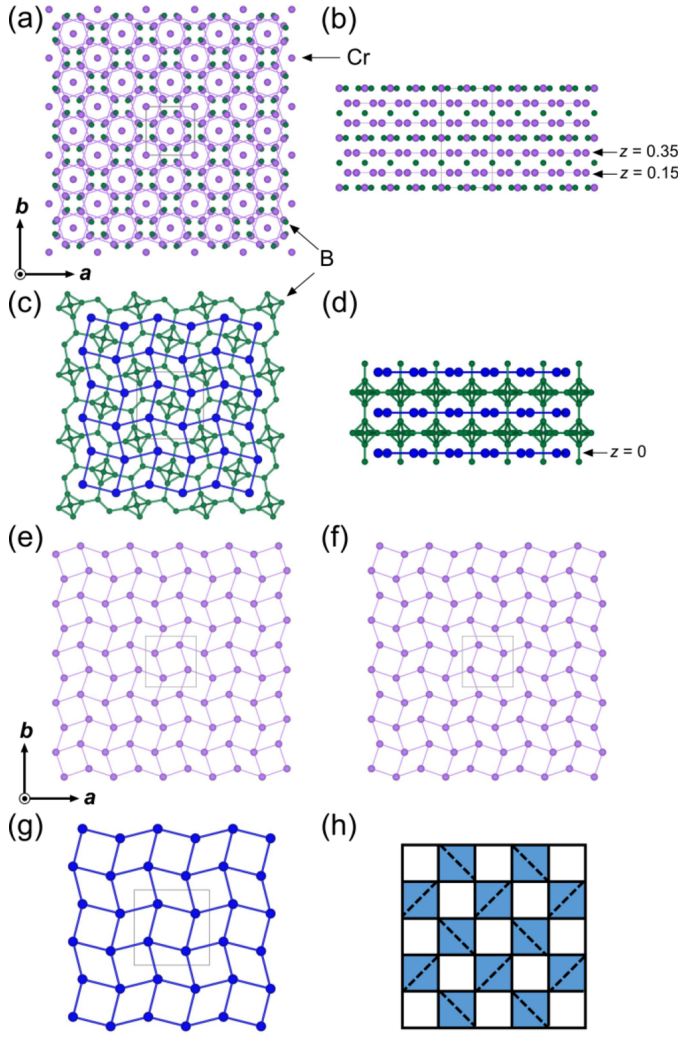

Figure 3
Crystal structures of binary metal borides: Cr_5B_3 (*a*, *b*) and TmB_4 (*c*, *d*) viewed along the *c*-axis (*a*, *c*) and *b*-axis (*b*, *d*) directions. Red, green and blue spheres indicate Cr, B and Tm atoms. Gray squares in (*a*, *c*, *e*, *f*, *g*) are respective unit cells. Cr lattices at z = 0.15 (*e*) and z = 0.35 (*f*) in Cr_5B_3. (*g*) Tm lattice at z = 0 in TmB_4. (*h*) Schematic of the SSL. The 1NN and the 2NN pairs are denoted by the solid and dashed lines, respectively.

square antiprisms around B1 site of Cr_5B_3 (in the right panel of Fig. 2) are illustrated. The distribution of Cr are clearly demonstrated by square and triangle tilting. This tilting geometrical feature, composed of squares and triangles, is found in the TmB_4 phase (Tm–Tm interatomic distances of 3.635 and 3.729 Å; Fisk *et al.*, 1972) (Fig. 3*g*) belonging to the UB_4-type structure (tetragonal, *P4/mbm*). Both the Cr_5B_3 and TmB_4 structures feature two-dimensional magnetic layers resembling the Shastry–Sutherland lattice (SSL), characterized by orthogonal dimers and interdimer interactions. However, while the SSL network in TmB_4 is isolated within the structure, the SSL in Cr_5B_3 are embedded in a three-dimensional framework, making the magnetic frustration more complex and less idealized. This tiling structure is known as the SSL (Shastry & Sutherland, 1981). A schematic of the SSL is shown in Fig. 3*h*. The first-nearest-neighbor (1NN) and second-nearest-neighbor (2NN) pairs are denoted by the gray and black lines, respectively. Frustrated magnetic behavior with magnetic order is expected in Cr_5B_3-type analogous intermetallic compounds consisting of SSL.

3. Synthesis and crystallization

Cr_5B_3 exhibits incongruent melting behavior during a peritectic reaction at 2247 K (Massalski *et al.*, 2016). Cr_5B_3 was obtained as a by-product of the synthesis of $YCrB_4$ crystals. The starting materials were Y (99.9%), Cr (99.95%), and B (99.5%). The samples were weighed at an atomic ratio Y:Cr:B = 1:7:4. The mixtures were then melted in an Ar arc melting furnace (ACM-01, Diavac). The resulting button-like product was then turned over and remelted thrice to improve its chemical homogeneity. Single crystals for the X-ray diffraction measurements were obtained from the fractured surface of this button-like product.

4. Refinement

The refinement process was conducted for the space-group type *I4/mcm* as described by Bertaut & Blum 1953. A correction for isotropic extinction was applied during the least-squares refinement. The final refinements were performed by applying the anisotropic ADPs to each atom. These final refinement results are listed in Table 3. The refinement was successful, with the *R* factor converging without any problems and no noticeable residuals.

Table 3
Experimental details.

Crystal data	
Chemical formula	Cr_5B_3
M_r	292.43
Crystal system, space group	Tetragonal, *I4/mcm*
Temperature (K)	294
a, *c* (Å)	5.47276 (5), 10.07939 (16)
V (Å^3)	301.89 (1)
Z	4
Radiation type	Mo *Kα*
μ (mm^{-1})	17.06
Crystal size (mm)	0.06 × 0.04 × 0.03
Data collection	
Diffractometer	XtaLAB Synergy, Dualflex, HyPix
Absorption correction	Gaussian (*CrysAlis PRO*; Rigaku OD, 2019)
T_{min}, T_{max}	0.520, 0.737
No. of measured, independent and observed [$I > 2\sigma(I)$] reflections	14650, 726, 687
R_{int}	0.032
(sin $\theta/\lambda)_{max}$ (Å^{-1})	1.273
Refinement	
$R[F^2 > 2\sigma(F^2)]$, $wR(F^2)$, *S*	0.011, 0.024, 1.10
No. of reflections	726
No. of parameters	16
$\Delta\rho_{max}$, $\Delta\rho_{min}$ (e Å^{-3})	0.61, −0.79

Computer programs: *CrysAlis PRO* (Rigaku OD, 2019), *SHELXT* (Sheldrick, 2015*a*), *SHELXL2016/6* (Sheldrick, 2015*b*) and *VESTA* (Momma & Izumi, 2011).

Funding information

We gratefully acknowledge the support from JSPS KAKENHI (grant Nos. JP19K05643, JP20H00189 and JP23K04373) and the GIMRT program (Nos. 202111-RDKGE-0002, 202211-RDKGE-0008, and 202311-RDKGE-0001) at the Institute for Materials Research, Tohoku University, Japan.

References

Bertaut, F. & Blum, P. (1953). *C. R. Hebd. Seances Acad. Sci.* **236**, 1055–1056.
Brandes, E. A. & Brook, G. B. (1992). *Smithells Metals Reference Book* pp. 4–41 Butterworth-Heinemann Ltd., Oxford, London.
Coleman, P. & Nevidomskyy, A. H. (2010). *J. Low Temp. Phys.* **161**, 182–202.
Corrêa, L. E., da Luz, M. S., de Lima, B. S., Cigarroa, O. V., da Silva, A. A. A. P., Coelho, G. C., Fisk, Z. & Machado, A. J. S. (2016). *J. Alloys Compd.* **660**, 44–47.
Cruceanu, E., Ivanciu, O. & Popa, M. (1975). *J. Less-Common Met.* **41**, 339–341.
Dahlqvist, M. & Rosen, J. (2022). *Mater. Adv.* **3**, 2908–2917.
Donohue, J. (1974). *The Structures of the Elements.* New York: Wiley.
Fisk, Z., Cooper, A. S., Schmidt, P. H. & Castellano, R. N. (1972). *Mater. Res. Bull.* **7**, 285–288.
Fukuma, M., Kawashima, K. & Akimitsu, J. (2012). *Phys. Procedia* **27**, 48–51.
Guy, C. N. (1976). *J. Phys. Chem. Solids* **37**, 1005–1009.
Guy, C. N. & Uraz, A. A. (1976). *J. Less-Common Met.* **48**, 199–203.
Hadi, M. A., Nasir, M. T., Roknuzzaman, M., Rayhan, M. A., Naqib, S. H. & Islam, A. K. M. A. (2016). *Phys. Status Solidi B* **253**, 2020–2026.
Hu, X. B., Zhu, Y. L., Sheng, N. C. & Ma, X. L. (2014). *Sci. Rep.* **4**, 7367.
Iizumi, K., Kudaka, K. & Okada, S. (1998). *J. Ceram. Soc. Japan* **106**, 931–934.
ICSD (2025). Inorganic Crystal Structure Database ICSD is available at FIZ Karlsruhe at https://icsd.fiz-karlsruhe.de/index.xhtml
Kageyama, H., Yoshimura, K., Stern, R., Mushnikov, N. V., Onizuka, K., Kato, M., Kosuge, K., Slichter, C. P., Goto, T. & Ueda, Y. (1999). *Phys. Rev. Lett.* **82**, 3168–3171.
Leyarovska, L., Leyarovski, E., Popov, C. & Midlarz, T. (1979). *J. Less-Common Met.* **67**, 389–398.
Lundström, T. (1969). *Ark. Kemi* **31**, 227–266.

Machado, A. J. S., Costa, A. M. S., Nunes, C. A., dos Santos, C. A. M., Grant, T. & Fisk, Z. (2011). *Solid State Commun.* **151**, 1445–1458.
Massalski, T., Okamoto, H., Subramanian, P. & Kacprzak, L. (2016). In *Binary Alloy Phase Diagrams*. Materials Park: ASM International.
McGuire, M. A. & Parker, D. S. (2016). *Phys. Rev. B* **93**, 064507.
Momma, K. & Izumi, F. (2011). *J. Appl. Cryst.* **44**, 1272–1276.
Okada, S., Kudou, K., Iizumi, K., Kudaka, K., Higashi, I. & Lundström, T. (1996). *J. Cryst. Growth* **166**, 429–435.
Paradelli, G. & Gianoglio, C. (1976). *Metallurgia Italiana* **68**, 191–194.
Portnoi, K. I., Romashov, V. M. & Romanovich, I. V. (1969). *Powder Metall. Met. Ceram.* **8**, 298–302.
Rigaku OD (2019). *CrysAlis PRO*. Rigaku Oxford Diffraction, Yarnton, England.
Robitsch, J. von (1974). *Arch. Lagerst. Ostalpen* **2**, 239–264.
Rogl, P. & Nowotny, H. (1978). *J. Less-Common Met.* **61**, 39–45.
Ruan, B. B., Yang, Q. S., Zhou, M. H., Chen, G. H. & Ren, Z. A. (2021). *J. Alloys Compd.* **868**, 159230.
Shastry, B. S. & Sutherland, B. (1981). *Physica* **108B**, 1069–1070.
Sheldrick, G. M. (2015*a*). *Acta Cryst.* A**71**, 3–8.
Sheldrick, G. M. (2015*b*). *Acta Cryst.* C**71**, 3–8.
Siemensmeyer, K., Wulf, E., Mikeska, H.-J., Flachbart, K., Gabáni, S., Mat'aš, S., Priputen, P., Efdokimova, A. & Shitsevalova, N. (2008). *Phys. Rev. Lett.* **101**, 177201.
Tokuda, M., Yubuta, K., Shishido, T. & Sugiyama, K. (2022). *Acta Cryst.* E**78**, 76–79.
Tokuda, M., Yubuta, K., Shishido, T. & Sugiyama, K. (2023). *Acta Cryst.* E**79**, 1072–1075.
Ueta, D., Iwata, Y., Kobayashi, R., Kuwahara, K., Masuda, T. & Itoh, S. (2024). *Phys. Rev. B* **109**, 205127.

supporting information

Acta Cryst. (2025). E**81**, 748-752 [https://doi.org/10.1107/S2056989025006437]

Cr_5B_3 with the Shastry–Sutherland lattices

Makoto Tokuda, Kunio Yubuta, Toetsu Shishido and Kazumasa Sugiyama

Computing details

Pentachromium triboride

Crystal data

Cr_5B_3
M_r = 292.43
Tetragonal, *I*4/*mcm*
a = 5.47276 (5) Å
c = 10.07939 (16) Å
V = 301.89 (1) Å^3
Z = 4
F(000) = 540
D_x = 6.434 Mg m^{-3}
Mo *Kα* radiation, *λ* = 0.71073 Å
Cell parameters from 8812 reflections
θ = 4.0–65.0°
μ = 17.06 mm^{-1}
T = 294 K
Block, metallic
0.06 × 0.04 × 0.03 mm

Data collection

XtaLAB Synergy, Dualflex, HyPix diffractometer
Radiation source: micro-focus sealed X-ray tube, PhotonJet (Mo) X-ray Source
Mirror monochromator
Detector resolution: 10.0000 pixels mm^{-1}
ω scans
Absorption correction: gaussian (CrysAlisPro; Rigaku OD, 2019)
T_{min} = 0.520, T_{max} = 0.737
14650 measured reflections
726 independent reflections
687 reflections with $I > 2\sigma(I)$
R_{int} = 0.032
θ_{max} = 64.8°, θ_{min} = 4.0°
h = −13→12
k = −12→13
l = −25→25

Refinement

Refinement on F^2
Least-squares matrix: full
$R[F^2 > 2\sigma(F^2)]$ = 0.011
$wR(F^2)$ = 0.024
S = 1.10
726 reflections
16 parameters
0 restraints
$w = 1/[\sigma^2(F_o^2) + (0.0099P)^2 + 0.1133P]$ where $P = (F_o^2 + 2F_c^2)/3$
$(\Delta/\sigma)_{max}$ = 0.001
$\Delta\rho_{max}$ = 0.61 e Å^{-3}
$\Delta\rho_{min}$ = −0.79 e Å^{-3}
Extinction correction: *SHELXL2016/6* (Sheldrick, 2015b), $Fc^*=kFc[1+0.001xFc^2\lambda^3/\sin(2\theta)]^{-1/4}$
Extinction coefficient: 0.0092 (5)

Special details

Geometry. All esds (except the esd in the dihedral angle between two l.s. planes) are estimated using the full covariance matrix. The cell esds are taken into account individually in the estimation of esds in distances, angles and torsion angles; correlations between esds in cell parameters are only used when they are defined by crystal symmetry. An approximate (isotropic) treatment of cell esds is used for estimating esds involving l.s. planes.

Fractional atomic coordinates and isotropic or equivalent isotropic displacement parameters (Å²)

	x	*y*	*z*	U_{iso}*/U_{eq}
Cr01	0.17128 (2)	0.67128 (2)	0.14618 (2)	0.00387 (2)
Cr02	0.000000	0.000000	0.000000	0.00391 (2)
B01	0.000000	0.000000	0.250000	0.00583 (12)
B02	0.38263 (10)	0.88263 (10)	0.000000	0.00492 (8)

Atomic displacement parameters (Å²)

	U^{11}	U^{22}	U^{33}	U^{12}	U^{13}	U^{23}
Cr01	0.00396 (2)	0.00396 (2)	0.00369 (2)	−0.00001 (1)	−0.00022 (1)	−0.00022 (1)
Cr02	0.00312 (2)	0.00312 (2)	0.00547 (4)	0.000	0.000	0.000
B01	0.00544 (17)	0.00544 (17)	0.0066 (3)	0.000	0.000	0.000
B02	0.00489 (12)	0.00489 (12)	0.0050 (2)	−0.00013 (15)	0.000	0.000

Geometric parameters (Å, º)

Cr01—B02^{i}	2.1803 (3)	Cr01—Cr01^{viii}	2.8098 (1)
Cr01—B02^{ii}	2.1803 (3)	Cr01—Cr01^{ix}	2.8098 (1)
Cr01—B02	2.2015 (6)	Cr01—Cr01^{x}	2.8688 (1)
Cr01—B01^{iii}	2.2826 (1)	Cr02—B02^{xi}	2.1903 (4)
Cr01—B01^{iv}	2.2826 (1)	Cr02—B02^{i}	2.1903 (4)
Cr01—Cr01^{v}	2.4218 (1)	Cr02—B02^{xii}	2.1903 (4)
Cr01—Cr02^{vi}	2.5072 (1)	Cr02—B02^{xiii}	2.1903 (4)
Cr01—Cr02^{iv}	2.5072 (1)	B02—B02^{xiv}	1.8168 (16)
Cr01—Cr01^{vii}	2.6513 (1)		
B02^{i}—Cr01—B02^{ii}	49.25 (4)	Cr01^{i}—Cr02—Cr01^{xvi}	71.983 (3)
B02^{i}—Cr01—B02	89.970 (13)	Cr01^{vii}—Cr02—Cr01^{xvi}	110.203 (2)
B02^{ii}—Cr01—B02	89.970 (13)	Cr01^{xv}—Cr02—Cr01^{xvi}	69.797 (2)
B02^{i}—Cr01—B01^{iii}	96.830 (19)	Cr01^{xiii}—Cr02—Cr01^{xvi}	110.203 (2)
B02^{ii}—Cr01—B01^{iii}	145.619 (18)	B02^{xi}—Cr02—Cr01^{xii}	125.194 (13)
B02—Cr01—B01^{iii}	96.230 (7)	B02^{i}—Cr02—Cr01^{xii}	54.806 (13)
B02^{i}—Cr01—B01^{iv}	145.619 (18)	B02^{xii}—Cr02—Cr01^{xii}	55.399 (13)
B02^{ii}—Cr01—B01^{iv}	96.830 (18)	B02^{xiii}—Cr02—Cr01^{xii}	124.601 (13)
B02—Cr01—B01^{iv}	96.230 (7)	Cr01^{xi}—Cr02—Cr01^{xii}	69.797 (2)
B01^{iii}—Cr01—B01^{iv}	115.923 (3)	Cr01^{i}—Cr02—Cr01^{xii}	110.203 (2)
B02^{i}—Cr01—Cr01^{v}	152.867 (17)	Cr01^{vii}—Cr02—Cr01^{xii}	71.983 (3)
B02^{ii}—Cr01—Cr01^{v}	152.867 (17)	Cr01^{xv}—Cr02—Cr01^{xii}	108.017 (3)
B02—Cr01—Cr01^{v}	101.803 (14)	Cr01^{xiii}—Cr02—Cr01^{xii}	180.0
B01^{iii}—Cr01—Cr01^{v}	57.961 (2)	Cr01^{xvi}—Cr02—Cr01^{xii}	69.797 (2)
B01^{iv}—Cr01—Cr01^{v}	57.961 (1)	B02^{xi}—Cr02—Cr01^{xvii}	55.399 (13)
B02^{i}—Cr01—Cr02^{vi}	55.184 (13)	B02^{i}—Cr02—Cr01^{xvii}	124.601 (13)
B02^{ii}—Cr01—Cr02^{vi}	94.138 (15)	B02^{xii}—Cr02—Cr01^{xvii}	54.806 (13)
B02—Cr01—Cr02^{vi}	54.980 (5)	B02^{xiii}—Cr02—Cr01^{xvii}	125.194 (13)
B01^{iii}—Cr01—Cr02^{vi}	63.279 (1)	Cr01^{xi}—Cr02—Cr01^{xvii}	71.983 (3)
B01^{iv}—Cr01—Cr02^{vi}	149.178 (3)	Cr01^{i}—Cr02—Cr01^{xvii}	108.017 (3)

Cr01^{v}—Cr01—Cr02^{vi}	112.681 (3)	Cr01^{vii}—Cr02—Cr01^{xvii}	69.797 (2)
B02^{i}—Cr01—Cr02^{iv}	94.138 (15)	Cr01^{xv}—Cr02—Cr01^{xvii}	110.203 (2)
B02^{ii}—Cr01—Cr02^{iv}	55.184 (13)	Cr01^{xiii}—Cr02—Cr01^{xvii}	69.797 (2)
B02—Cr01—Cr02^{iv}	54.980 (5)	Cr01^{xvi}—Cr02—Cr01^{xvii}	180.0
B01^{iii}—Cr01—Cr02^{iv}	149.178 (3)	Cr01^{xii}—Cr02—Cr01^{xvii}	110.203 (2)
B01^{iv}—Cr01—Cr02^{iv}	63.279 (1)	Cr01^{xvii}—B01—Cr01^{viii}	149.038 (3)
Cr01^{v}—Cr01—Cr02^{iv}	112.681 (3)	Cr01^{xvii}—B01—Cr01^{xiii}	77.867 (1)
Cr02^{vi}—Cr01—Cr02^{iv}	101.022 (3)	Cr01^{viii}—B01—Cr01^{xiii}	131.507 (3)
B02^{i}—Cr01—Cr01^{vii}	52.552 (7)	Cr01^{xvii}—B01—Cr01^{iii}	131.507 (3)
B02^{ii}—Cr01—Cr01^{vii}	52.552 (7)	Cr01^{viii}—B01—Cr01^{iii}	77.867 (2)
B02—Cr01—Cr01^{vii}	137.988 (14)	Cr01^{xiii}—B01—Cr01^{iii}	64.078 (3)
B01^{iii}—Cr01—Cr01^{vii}	105.481 (2)	Cr01^{xvii}—B01—Cr01^{xviii}	64.078 (3)
B01^{iv}—Cr01—Cr01^{vii}	105.481 (2)	Cr01^{viii}—B01—Cr01^{xviii}	125.425 (3)
Cr01^{v}—Cr01—Cr01^{vii}	120.209 (3)	Cr01^{xiii}—B01—Cr01^{xviii}	75.975 (4)
Cr02^{vi}—Cr01—Cr01^{vii}	104.063 (2)	Cr01^{iii}—B01—Cr01^{xviii}	77.867 (1)
Cr02^{iv}—Cr01—Cr01^{vii}	104.063 (2)	Cr01^{xvii}—B01—Cr01^{i}	125.425 (3)
B02^{i}—Cr01—Cr01^{viii}	91.142 (10)	Cr01^{viii}—B01—Cr01^{i}	64.078 (3)
B02^{ii}—Cr01—Cr01^{viii}	114.398 (7)	Cr01^{xiii}—B01—Cr01^{i}	77.867 (2)
B02—Cr01—Cr01^{viii}	148.111 (6)	Cr01^{iii}—B01—Cr01^{i}	75.975 (4)
B01^{iii}—Cr01—Cr01^{viii}	52.013 (2)	Cr01^{xviii}—B01—Cr01^{i}	149.038 (3)
B01^{iv}—Cr01—Cr01^{viii}	100.625 (3)	Cr01^{xvii}—B01—Cr01^{xix}	75.975 (4)
Cr01^{v}—Cr01—Cr01^{viii}	66.026 (4)	Cr01^{viii}—B01—Cr01^{xix}	77.867 (1)
Cr02^{vi}—Cr01—Cr01^{viii}	100.852 (2)	Cr01^{xiii}—B01—Cr01^{xix}	149.038 (3)
Cr02^{iv}—Cr01—Cr01^{viii}	156.417 (2)	Cr01^{iii}—B01—Cr01^{xix}	125.425 (3)
Cr01^{vii}—Cr01—Cr01^{viii}	61.849 (1)	Cr01^{xviii}—B01—Cr01^{xix}	77.867 (1)
B02^{i}—Cr01—Cr01^{ix}	114.398 (7)	Cr01^{i}—B01—Cr01^{xix}	131.507 (3)
B02^{ii}—Cr01—Cr01^{ix}	91.142 (10)	Cr01^{xvii}—B01—Cr01^{vii}	77.867 (2)
B02—Cr01—Cr01^{ix}	148.111 (6)	Cr01^{viii}—B01—Cr01^{vii}	75.975 (4)
B01^{iii}—Cr01—Cr01^{ix}	100.625 (3)	Cr01^{xiii}—B01—Cr01^{vii}	125.425 (3)
B01^{iv}—Cr01—Cr01^{ix}	52.013 (2)	Cr01^{iii}—B01—Cr01^{vii}	149.038 (3)
Cr01^{v}—Cr01—Cr01^{ix}	66.026 (4)	Cr01^{xviii}—B01—Cr01^{vii}	131.507 (3)
Cr02^{vi}—Cr01—Cr01^{ix}	156.417 (2)	Cr01^{i}—B01—Cr01^{vii}	77.867 (2)
Cr02^{iv}—Cr01—Cr01^{ix}	100.852 (2)	Cr01^{xix}—B01—Cr01^{vii}	64.078 (3)
Cr01^{vii}—Cr01—Cr01^{ix}	61.849 (2)	Cr01^{xvii}—B01—Cr02^{xx}	117.287 (2)
Cr01^{viii}—Cr01—Cr01^{ix}	56.302 (3)	Cr01^{viii}—B01—Cr02^{xx}	62.713 (2)
B02^{i}—Cr01—Cr01^{x}	110.285 (13)	Cr01^{xiii}—B01—Cr02^{xx}	117.287 (2)
B02^{ii}—Cr01—Cr01^{x}	137.034 (5)	Cr01^{iii}—B01—Cr02^{xx}	62.713 (2)
B02—Cr01—Cr01^{x}	48.782 (11)	Cr01^{xviii}—B01—Cr02^{xx}	62.713 (2)
B01^{iii}—Cr01—Cr01^{x}	51.067 (1)	Cr01^{i}—B01—Cr02^{xx}	117.287 (2)
B01^{iv}—Cr01—Cr01^{x}	98.917 (3)	Cr01^{xix}—B01—Cr02^{xx}	62.713 (2)
Cr01^{v}—Cr01—Cr01^{x}	63.500 (3)	Cr01^{vii}—B01—Cr02^{xx}	117.287 (2)
Cr02^{vi}—Cr01—Cr01^{x}	55.102 (1)	Cr01^{xvii}—B01—Cr02	62.713 (2)
Cr02^{iv}—Cr01—Cr01^{x}	98.112 (3)	Cr01^{viii}—B01—Cr02	117.287 (2)
Cr01^{vii}—Cr01—Cr01^{x}	152.478 (2)	Cr01^{xiii}—B01—Cr02	62.713 (2)
Cr01^{viii}—Cr01—Cr01^{x}	101.560 (1)	Cr01^{iii}—B01—Cr02	117.287 (2)
Cr01^{ix}—Cr01—Cr01^{x}	129.526 (3)	Cr01^{xviii}—B01—Cr02	117.287 (2)
B02^{xi}—Cr02—B02^{i}	180.0	Cr01^{i}—B01—Cr02	62.713 (2)
B02^{xi}—Cr02—B02^{xii}	90.0	Cr01^{xix}—B01—Cr02	117.287 (2)

B02^{i}—Cr02—B02^{xii}	90.0	Cr01^{vii}—B01—Cr02	62.713 (2)
B02^{xi}—Cr02—B02^{xiii}	90.0	Cr02^{xx}—B01—Cr02	180.0
B02^{i}—Cr02—B02^{xiii}	90.0	B02^{xiv}—B02—Cr01^{x}	65.376 (19)
B02^{xii}—Cr02—B02^{xiii}	180.00 (3)	B02^{xiv}—B02—Cr01^{xxi}	65.376 (19)
B02^{xi}—Cr02—Cr01^{xi}	55.399 (13)	Cr01^{x}—B02—Cr01^{xxi}	74.894 (14)
B02^{i}—Cr02—Cr01^{xi}	124.601 (13)	B02^{xiv}—B02—Cr01^{xxii}	65.376 (19)
B02^{xii}—Cr02—Cr01^{xi}	54.806 (13)	Cr01^{x}—B02—Cr01^{xxii}	130.75 (4)
B02^{xiii}—Cr02—Cr01^{xi}	125.194 (13)	Cr01^{xxi}—B02—Cr01^{xxii}	85.031 (16)
B02^{xi}—Cr02—Cr01^{i}	124.601 (13)	B02^{xiv}—B02—Cr01^{xxiii}	65.376 (19)
B02^{i}—Cr02—Cr01^{i}	55.399 (13)	Cr01^{x}—B02—Cr01^{xxiii}	85.031 (16)
B02^{xii}—Cr02—Cr01^{i}	125.194 (13)	Cr01^{xxi}—B02—Cr01^{xxiii}	130.75 (4)
B02^{xiii}—Cr02—Cr01^{i}	54.806 (13)	Cr01^{xxii}—B02—Cr01^{xxiii}	74.894 (14)
Cr01^{xi}—Cr02—Cr01^{i}	180.0	B02^{xiv}—B02—Cr02^{iv}	117.946 (18)
B02^{xi}—Cr02—Cr01^{vii}	125.194 (13)	Cr01^{x}—B02—Cr02^{iv}	137.087 (3)
B02^{i}—Cr02—Cr01^{vii}	54.806 (13)	Cr01^{xxi}—B02—Cr02^{iv}	70.010 (2)
B02^{xii}—Cr02—Cr01^{vii}	55.399 (13)	Cr01^{xxii}—B02—Cr02^{iv}	70.010 (2)
B02^{xiii}—Cr02—Cr01^{vii}	124.601 (13)	Cr01^{xxiii}—B02—Cr02^{iv}	137.087 (3)
Cr01^{xi}—Cr02—Cr01^{vii}	110.203 (2)	B02^{xiv}—B02—Cr02^{vi}	117.946 (18)
Cr01^{i}—Cr02—Cr01^{vii}	69.797 (2)	Cr01^{x}—B02—Cr02^{vi}	70.010 (2)
B02^{xi}—Cr02—Cr01^{xv}	54.806 (13)	Cr01^{xxi}—B02—Cr02^{vi}	137.087 (3)
B02^{i}—Cr02—Cr01^{xv}	125.194 (13)	Cr01^{xxii}—B02—Cr02^{vi}	137.087 (3)
B02^{xii}—Cr02—Cr01^{xv}	124.601 (13)	Cr01^{xxiii}—B02—Cr02^{vi}	70.010 (2)
B02^{xiii}—Cr02—Cr01^{xv}	55.399 (13)	Cr02^{iv}—B02—Cr02^{vi}	124.11 (4)
Cr01^{xi}—Cr02—Cr01^{xv}	69.797 (2)	B02^{xiv}—B02—Cr01	137.989 (14)
Cr01^{i}—Cr02—Cr01^{xv}	110.203 (2)	Cr01^{x}—B02—Cr01	81.796 (6)
Cr01^{vii}—Cr02—Cr01^{xv}	180.0	Cr01^{xxi}—B02—Cr01	81.796 (6)
B02^{xi}—Cr02—Cr01^{xiii}	54.806 (13)	Cr01^{xxii}—B02—Cr01	139.630 (18)
B02^{i}—Cr02—Cr01^{xiii}	125.194 (13)	Cr01^{xxiii}—B02—Cr01	139.630 (18)
B02^{xii}—Cr02—Cr01^{xiii}	124.601 (13)	Cr02^{iv}—B02—Cr01	69.622 (17)
B02^{xiii}—Cr02—Cr01^{xiii}	55.399 (13)	Cr02^{vi}—B02—Cr01	69.622 (17)
Cr01^{xi}—Cr02—Cr01^{xiii}	110.203 (2)	B02^{xiv}—B02—Cr01^{xxiv}	137.989 (14)
Cr01^{i}—Cr02—Cr01^{xiii}	69.797 (2)	Cr01^{x}—B02—Cr01^{xxiv}	139.630 (18)
Cr01^{vii}—Cr02—Cr01^{xiii}	108.017 (3)	Cr01^{xxi}—B02—Cr01^{xxiv}	139.630 (18)
Cr01^{xv}—Cr02—Cr01^{xiii}	71.983 (3)	Cr01^{xxii}—B02—Cr01^{xxiv}	81.796 (6)
B02^{xi}—Cr02—Cr01^{xvi}	124.601 (13)	Cr01^{xxiii}—B02—Cr01^{xxiv}	81.796 (6)
B02^{i}—Cr02—Cr01^{xvi}	55.399 (13)	Cr02^{iv}—B02—Cr01^{xxiv}	69.622 (17)
B02^{xii}—Cr02—Cr01^{xvi}	125.194 (13)	Cr02^{vi}—B02—Cr01^{xxiv}	69.622 (17)
B02^{xiii}—Cr02—Cr01^{xvi}	54.806 (13)	Cr01—B02—Cr01^{xxiv}	84.02 (3)
Cr01^{xi}—Cr02—Cr01^{xvi}	108.017 (3)		

Symmetry codes: (i) $-y+1, x, z$; (ii) $y-1, -x+1, -z$; (iii) $-x+1/2, -y+1/2, -z+1/2$; (iv) $x, y+1, z$; (v) $-x+1/2, -y+3/2, -z+1/2$; (vi) $-x+1/2, y+1/2, -z$; (vii) $-x, -y+1, z$; (viii) $y-1/2, -x+1/2, -z+1/2$; (ix) $-y+1/2, x+1/2, -z+1/2$; (x) $y, -x+1, z$; (xi) $y-1, -x, -z$; (xii) $-x, -y+1, -z$; (xiii) $x, y-1, z$; (xiv) $-x+1, -y+2, -z$; (xv) $x, y-1, -z$; (xvi) $-y+1, x, -z$; (xvii) $y-1, -x, z$; (xviii) $-y+1/2, x-1/2, -z+1/2$; (xix) $x-1/2, y-1/2, -z+1/2$; (xx) $-x, y, -z+1/2$; (xxi) $-y+1, x+1, z$; (xxii) $-y+1, x+1, -z$; (xxiii) $y, -x+1, -z$; (xxiv) $x, y, -z$.